(Received 9 July 2025, Accepted 20 August 2025, Scheduled 29 August 2025)

Compact Arrow-Shaped Half-Mode Substrate Integrated Waveguide (SIW) Self-Diplexed Antenna for X/Ku-Bands

Bhim S. Singla[1], Ashish Kumar[2], Mohammad S. Zidan[3,4], Zahriladha Zakaria[5], and Ahmed J. A. Al-Gburi[5,*]

[1]*Department of Computer Science, Punjabi University Neighbourhood Campus, Ralla-151510, Punjab, India*
[2]*Chitkara University Institute of Engineering and Technology, Chitkara University, Punjab, India*
[3]*Department of Electrical, Electronic and Systems Engineering, Faculty of Engineering and Built Environment Universiti Kebangsaan Malaysia, Bangi 43600, Selangor, Malaysia*
[4]*Technical Institute of Anbar, Middle Technical University, Iraq*
[5]*Center for Telecommunication Research & Innovation (CeTRI) Fakulti Teknologi dan Kejuruteraan Elektronik dan Komputer (FTKEK) Universiti Teknikal Malaysia Melaka (UTeM), Durian Tunggal, Melaka 76100, Malaysia*

ABSTRACT: This article presents a compact, triple-band half mode substrate integrated waveguide (HMSIW) based self-multiplexing antenna (SMA) designed for various X-/Ku-band applications. The proposed SMA comprises a compact HMSIW with slots of unequal widths excited with three different ports resembling the anatomy of an arrow. These three slots are driven by a 50 Ω microstrip line feed, facilitating radiations at 10.82, 12.28, and 13.95 GHz with good isolation between the ports. Independent functioning at three different frequency bands is made possible by the remarkable versatility of the proposed SMA design method. With the isolation of nearly 20 dB between ports and gains of 3.97, 4.62, and 7.55 dBi at ports resonating at three distinct frequencies, the SMA-HMSIW element's total arrangement allows for a small antenna size of $0.44\lambda_g^2$ at the lowest frequency of operation. The proposed SMA structure has been fabricated, and the results are measured which show good agreement with simulated ones.

1. INTRODUCTION

In the rapid development in the next-generation wireless technologies and demand of multistranded systems, the design and performance parameters of antennas become more rigid [1, 2]. Multiband antennas for general usage must be small and light, have improved radiating elements, and be simple to integrate in order to achieve these goals. Multi-band operations were previously conducted using one port multiband antennas [3, 4]. These antennas are only capable of sending and receiving data; they are unable to accomplish both simultaneously. For data to be transmitted and received independently, an external multiplexer is necessary; however, this adds complexity and space to the system with poor isolation. To overcome these issues, self-multiplexing antenna (SMA) comes into picture which can resonate at multiple frequencies without the use of multiplexer and hence provide simpler solution with compact antenna size [5]. Moreover, because of its high-Q factors, one-directional pattern, and high gains, substrate integrated waveguide (SIW) antennas have recently become a viable option for high-performance communication [6]. Along with multistranded systems, there is also the requirement of high data rate, which can be accomplished with multi-input multi-output (MIMO) technology [7]. In rich scattering situations, MIMO technology successfully mitigates multipath fading while improving channel capacity, reliability, and spectral efficiency. Numerous SMA designs have been reported in the literature utilizing various structures in non-planar form, multilayer structure, etc. However, SIW technique has made it feasible to design SMAs on a planar structure with high efficiency, broadside radiation pattern, improved front to back ratio, etc. For instance, in [8] the authors present a novel, compact, triple-fed, high-isolation, self-triplexing antenna based on a SIW. The antenna is designed with three planar ports and an I-shaped slot to enable operation at three distinct frequencies (4.14, 6.1, and 8.32 GHz) while maintaining isolation above 30.8 dB. In another article [9], the authors present a self-triplexing antenna based on a SIW cavity, designed for C- and X-band applications. It utilizes a novel nonlinear replicated hybrid slot (NLR-HS) to achieve three distinct resonances at 5.23 GHz, 7.50 GHz, and 10.82 GHz, with high isolation ($>$ 40 dB) and good gain (6.28–7.33 dBi). Further in [10], a novel self-triplexing SIW cavity-backed slot antenna designed for multiband communication systems is presented. It operates at three distinct frequencies (6.53, 7.65, and 9.09 GHz) with excellent isolation ($>$ 18 dB) using a simple microstrip feeding network. Apart from the triple band configuration, other designs like diplexing [11, 12], quadruplexing [14, 15], hexaplexing [16], and octaplexing antennas [17] have been explored by various researchers. However, conventional SIW-based SMA provides excellent isolation and performance parameters, but still full mode SIW (FMSIW) occupies large

* Corresponding author: Ahmed Jamal Abdullah Al-Gburi (ahmedjamal@ieee.org, ahmedjamal@utem.edu.my).

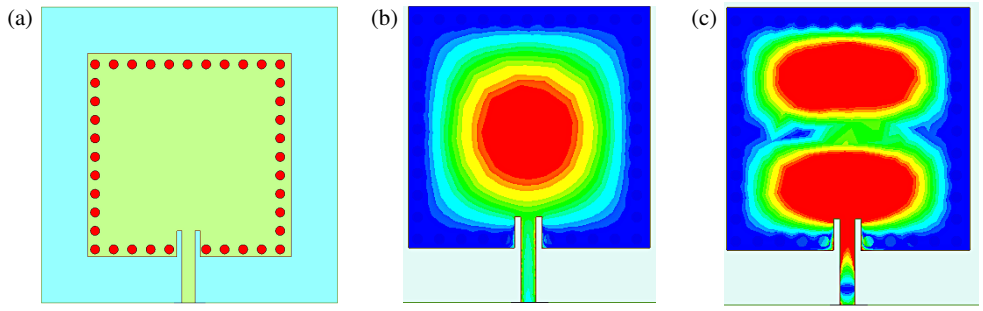

FIGURE 1. Full mode square SIW cavity depicting TE,110 and TE,120 modes.

space; therefore, some researchers have presented HMSIW and quarter mode SIW (QMISW) while retaining the performance of FMSIW. In such attempts, the authors in [18] introduce a novel QMSIW, derived by bisecting a half-mode SIW and investigate its use in antenna design. The proposed QMSIW preserves key electromagnetic properties of the original SIW while offering a more compact structure, enabling both linearly and circularly polarized radiations depending on the excitation mode. Further, [19] presents a compact, circularly polarized antenna based on a QMSIW sub-array using an isosceles right triangular cavity, and finally authors in [20] present a wideband HMSIW cavity-backed slot antenna designed on a cork substrate, targeting the full 5 GHz band. The literature also provides comprehensive study about SIW MIMO antenna design. For example, the authors in [21] present a compact dual-band 2×2 MIMO antenna-diplexer using HMSIW technology, operating at $\sim$ 3.4 GHz and $\sim$ 4.3 GHz with a 50% bandwidth enhancement via slot-loaded cavities. Further, [22] presents a compact dual-band 2×2 MIMO antenna based on HMSIW, achieving dual-band operation through proximity-coupled rectangular patches. The authors in [23] present a compact, dual-band 4-port MIMO antenna-diplexer designed using QMSIW technology for WLAN applications.

This work presents a novel SMA architecture based on an HMSIW cavity structure, utilizing an unexplored design strategy implemented for the targeted frequency bands to the best of our knowledge. The design presents a triple band SMA structure, contributing both miniaturization and independent frequency tunability. The manuscript is structured as follows. Section 2 details the design analysis of an HMSIW based SMA including the dimensional description of the proposed design. Section 3 focuses on the analysis of scattering parameters of the proposed design with the help of current distributions. Section 4 presents the phenomenon of the independent tunability of the frequency with the excitation of corresponding ports followed by the conclusion in Section 5.

2. DESIGN AND ANALYSIS OF PROPOSED SIW SELF-DIPLEXING ANTENNA

The proposed design is initiated with an FMSIW cavity of size 22 mm $\times$ 22 mm $\times$ 1.57 mm as depicted in Figure 1(a). The cavity has been analyzed with current distribution which shows that the conventional FMSIW operating at TE,110 mode and TE,120 mode is evaluated employing Eq. (1), a formula in [23], as depicted in Figures 1(b) and (c). The proposed structure has been developed on Rogers/RT duroid 5880 substrates with $\varepsilon_r = 2.2$, $h = 1.57$ mm, and $\tan\delta = 0.0012$. The reason behind the selection of this material is its low dielectric constant and loss tangent which reduces surface wave losses and ensures minimum dielectric losses. Moreover, the selected material has excellent dimensional stability with high frequency compatibility and ease of fabrication along with proven industry standards.

$$f_{mn0}^{FMSIW} = \frac{1}{2\pi\sqrt{\varepsilon_r}}\sqrt{\left(\frac{m\pi}{W_e^{FMSIW}}\right)^2 + \left(\frac{n\pi}{L_e^{FMSIW}}\right)^2} \quad (1)$$

$$\begin{cases} W_e^{FMSIW} = W - 1.08\frac{d^2}{s} + 0.1\frac{d^2}{W} \\ L_e^{FMSIW} = L - 1.08\frac{d^2}{s} + 0.1\frac{d^2}{L} \end{cases} \quad (2)$$

where $m = 1, 2, \ldots, n = 1, 2, \ldots, \mu$ is the relative permeability, and ε is the relative permittivity of the substrate. Further, the diameters of the vias and the spacing between them is chosen according to $s \leq 2d$ which leads to the reduction in the leakage.

Further to achieve the multiband characteristics, steps have been followed as shown in Figure 2. Interestingly, the final iteration is an arrow-like slot configuration, which was inadvertently produced by methodical optimization for performance, isolation, and compactness, and was later named because it resembles a arrow like structure. Initially, in the design steps, the FMSIW is designed to operate in TE,110 and TE,120 modes with electric field distribution as depicted in Figure 2(a). Then, FMSIW is bisected along magnetic wall, and one mode of TE,120 is cut into half forming two equal HMSIWs as shown in Figure 2(b). The huge size of the FMSIW cavity, which made it difficult to integrate into small devices, was the primary cause of the switch from FMSIW to HMSIW. The HMSIW structure reduced the size of the FMSIW cavity by around 50% by cutting it in half along its magnetic wall. Further, to achieve the multi-resonating frequencies, the HMSIW has been fed with other two feed lines opposite to each other and a slot in the center of the cavity as depicted in Figure 2(c). However, from the analysis of scattering parameters (discussed later), it has been found that port 2 and port 3 generate the same resonating frequency; therefore, two slanted slots have been added with the center slot in order to make it an arrow shaped structure as shown in Figure 2(d). Further, the lengths and widths of the slots have been optimized to achieve the required resonating frequencies with

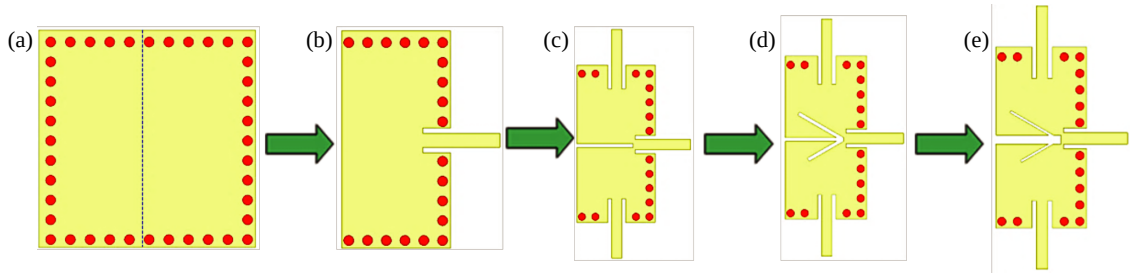

FIGURE 2. Iterative design progression of the suggested HMSIW-SMA.

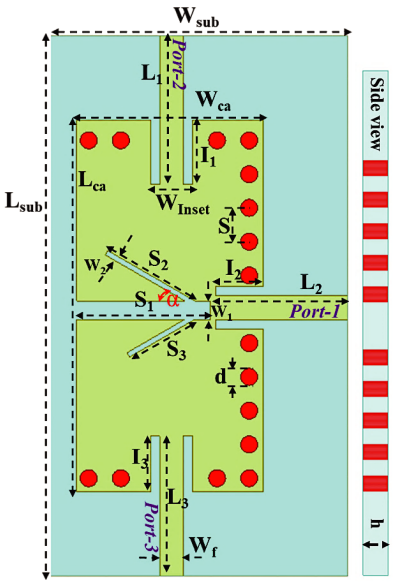

FIGURE 3. Dimensional layout of the modelled design. [Design parameters (Unit: mm): $L_{sub} = 32$, $W_{sub} = 17$, $L_{ca} = 22$, $W_{ca} = 11$, $L_1 = 8.8$, $L_2 = 7.8$, $L_3 = 8.3$, $I_1 = 3.8$, $I_2 = 2.8$, $I_3 = 3.3$, $W_f = 1.4$, $W_{inset} = 2.5$, $S = 2$, $d = 1$, $S_1 = 7.9$, $S_2 = 6.9$, $S_3 = 5.4$, $W_1 = 1.1$, $W_2 = 0.3$, $\alpha = 30°$, $h = 1.57$].

excellent impedance matching and isolation among the ports respectively as shown in Figure 2(e). The dimensional pictorial view of the proposed HMSIW is illustrated in Figure 3, which depicts the miniaturized size of 32 mm × 17 mm × 1.57 mm.

3. ANALYSIS OF SCATTERING PARAMETERS OF THE PROPOSED DESIGN

The scattering parameters of all the design steps are shown in Figure 4, in which square cavity shows dual-band characteristics at dominant mode i.e., TE,110 mode and second mode of operation, i.e., TE,120. The dominant mode resonates at 7.33 GHz with impedance matching S_{11}(dB) $= -13.7$ dB, and second order mode resonates at 11.48 GHz with low impedance matching S_{11}(dB) $= -4.5$ dB. Further, the higher mode has been cut into half and achieved HMSIW, and the resonating frequency shifted from 11.48 GHz to 13.67 GHz with S_{11}(dB) $= -31$ dB and impedance bandwidth $\approx$ 700 MHz as shown in Figure 4(a). This is because the size of the cavity has been reduced which causes the shifting of frequency on the higher side. In the next step, the HMSIW is fed with the 3 feed lines, and it can be observed from Figure 4(b) that port 2 and port 3 resonate at the same frequency, i.e., 12.3 GHz with S_{11}(dB) ≈ -17 dB and impedance bandwidth $\approx$ 420 MHz. The resonance frequencies occur at TE,210 mode of operation as depicted by the current distribution in the same figure. The red area shows equal portion of the current on both the halves. Next, the variation in the resonating frequency bands has been achieved with the addition of two slanted slots at $\alpha = 30°$ as shown in Figure 4(c), which depicts that the resonating frequencies of port 2 and port 3 have been shifted apart by 2.05 GHz with very low impedance matching and bandwidth at 10.75 GHz (port 2—red curve) but excellent impedance bandwidth and matching at other two frequencies i.e., 12.8 GHz (port 3—blue curve) and 14.02 GHz (port 1—black curve). Both the phenomena have also been verified by the corresponding current distribution. The current is more concentrated near the ports in green and light blue shaded area and near slots in red area. Still there are some issues in the responses received in Figure 4(c) which includes low impedance bandwidth and matching at 10.75 GHz and nonuniform gap (frequency ratio f_r) between the resonating frequencies of all the ports ($P2 : P3 = 2.05$ GHz ($f_r = 1.19$); $P1 : P3 = 1.22$ GHz ($f_r = 1.09$)). These issues have been addressed by optimizing the width of the slots, and the corresponding results are shown in Figure 4(d). The figure depicts the resonance at triple band frequencies, i.e., first band at 13.95 GHz (13.55–14.37 GHz) for port 1, second band at 10.82 GHz (10.91–10.71 GHz) for port 2, and third band at 12.28 GHz (12.11–12.46 GHz) for port 3. The scattering parameters of the proposed design (final step) has achieved excellent impedance matching at all the operating frequencies and equal frequency ratio $f_r = 1.13$. All the phenomena have been verified by the current distribution for all the frequencies. For port 1, TE,120 mode is responsible, and for Port 2 and Port 3, TE,210 mode is active with more current distribution near the corresponding resonating frequencies. From current distribution, it is evident that all the ports are independent from each other which can also be verified by the transmission coefficients expressed in Figure 4(e).

4. INDEPENDENT FREQUENCY TUNABILITY

The proposed design facilitates each independent frequency tuning with the variation of corresponding design parameters. For instance, by optimizing the length of the slot (S_2) from 3.4 mm to 5.4 mm, while maintaining other parameters constant, port 2 frequency, i.e., $f_2 = 10.82$, can be tuned from 10.4 to 11.8 GHz as depicted in Figure 5(a). Notably, the iso-

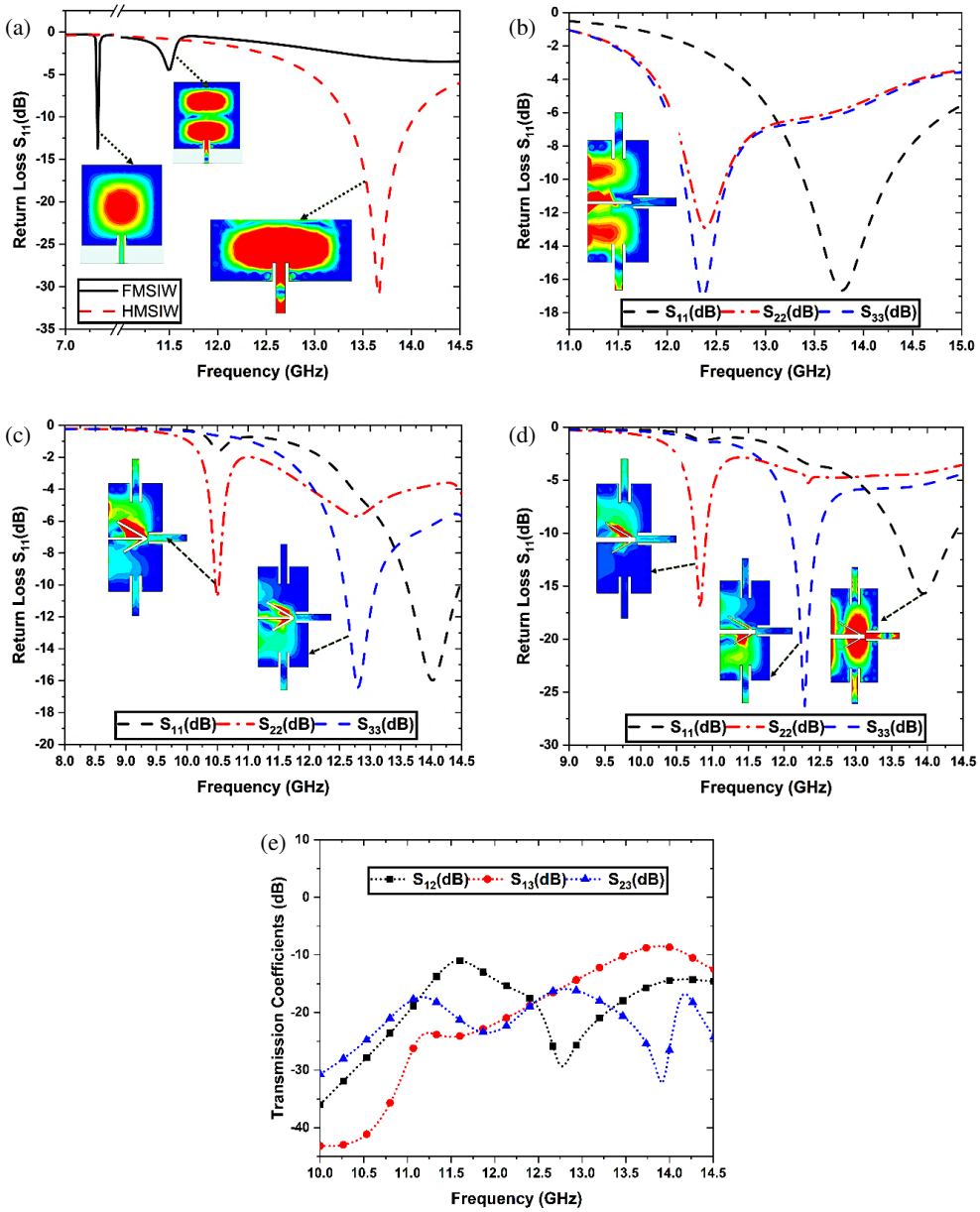

FIGURE 4. Scattering parameter analysis of the each step of the proposed HMSIW-SMA. (a) Comparison on FMSIW and HMSIW. (b) HMSIW with 3-ports with Horizontal slot. (c) HMSIW with equal width of arrow shaped slots. (d) HMSIW with unequal width of slots. (e) Transmission coefficients.

lation corresponding to the shift in the f_2 due to the changing parameter S_2 is not shown in the figure for brevity. Similarly, Figure 5(b) illustrates the same approach for tuning f_3 which can be adjusted from 11.25 to 13 GHz by changing parameters S_3 as shown in Figure 5(b). It is possible to achieve these frequency adjustments without changing the original cavity size. As a result, these adjustments barely affect the cavity's characteristics like leakage, efficiency, etc. f_2 and f_3 achieve the shifting ranges of 12.5% (10.57–11.9 GHz) and 15.8% (11.2–12.97 GHz), respectively. The antenna sustains consistent resonance and dependable performance with minor modifications to the slot parameters (S_2 and S_3), even in the presence of different loading circumstances or in close proximity to things. Further, Figure 5(c) depicts the variation in the isolation (S_{23}(dB)) with the width of tilted slots, and it has been observed that by varying the W_2 from 0.2 mm to 1 mm, the isolation between ports varies accordingly. Therefore, by considering the lowest value of the isolation at the resonant frequency bands, the optimized value of W_2 has been chosen. Furthermore, simulated 3D gain polar plot at the corresponding resonant frequencies is shown in Figure 6, which depicts the peak gain 7.5, 3.97, and 4.62 dBi at 13.95, 10.82, and 12.28 GHz, respectively. The shape of the pattern has been considerably impacted by the current distribution as depicted in Figure 4(d). For instance, at 13.95 GHz, the 3D polar plot shows maximum radiations on both sides of the centre slot, and one full portion of current can be observed due to TE,120 mode; therefore, the gain value is more than other frequencies. Further, at 10.82 & 12.28 GHz,

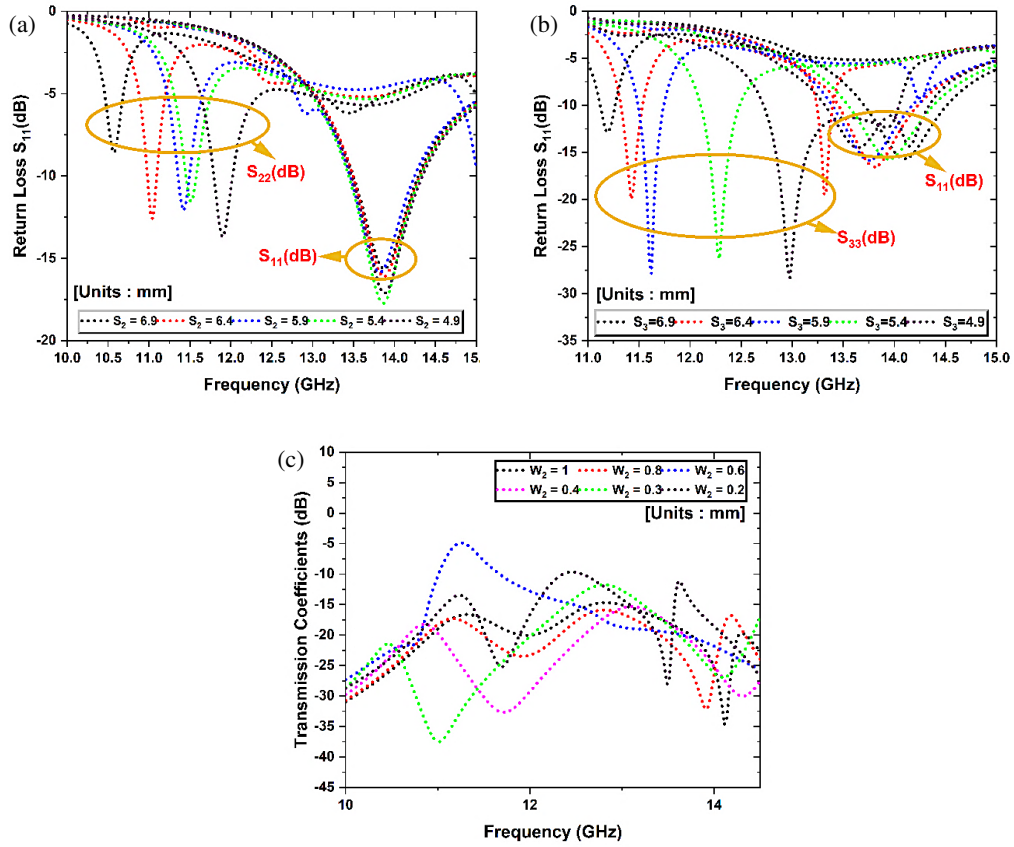

FIGURE 5. Frequency tunability and isolation controlling varying the lengths and width of the slots. (a) S_2 from 6.9 mm to 4.9 mm. (b) S_3 from 6.9 mm to 4.9 mm. (c) W_2 from 1 mm to 0.2 mm.

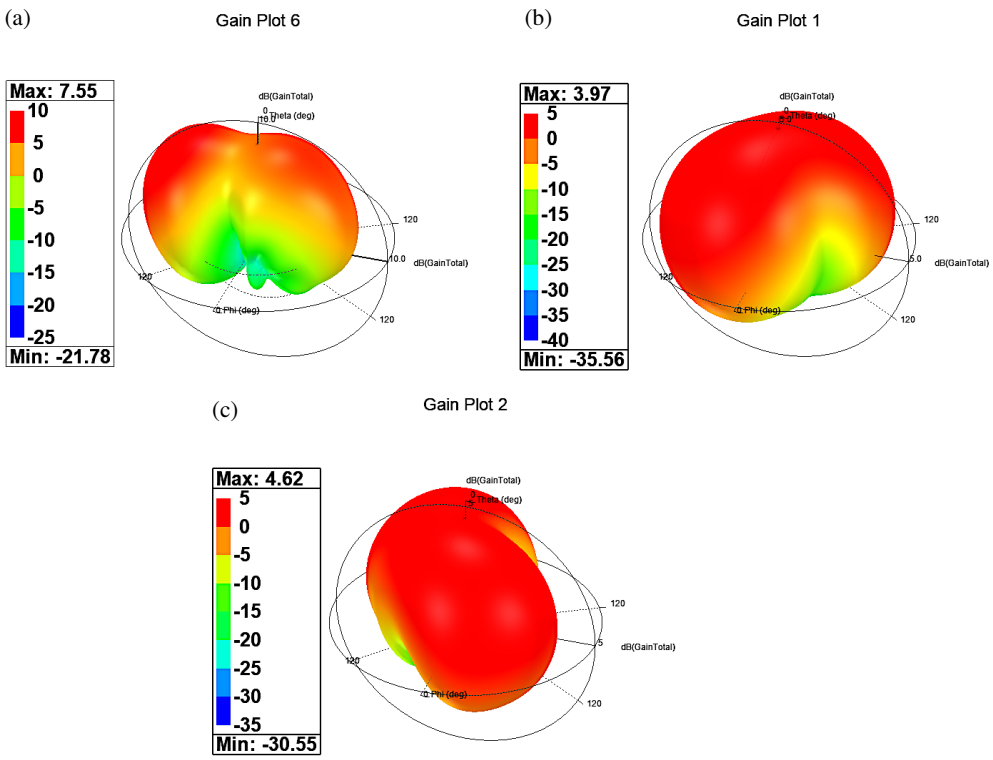

FIGURE 6. 3D gain polar plot of the proposed HMSIW-SMA at (a) 13.95 GHz, (b) 10.82 GHz, (c) 12.28 GHz.

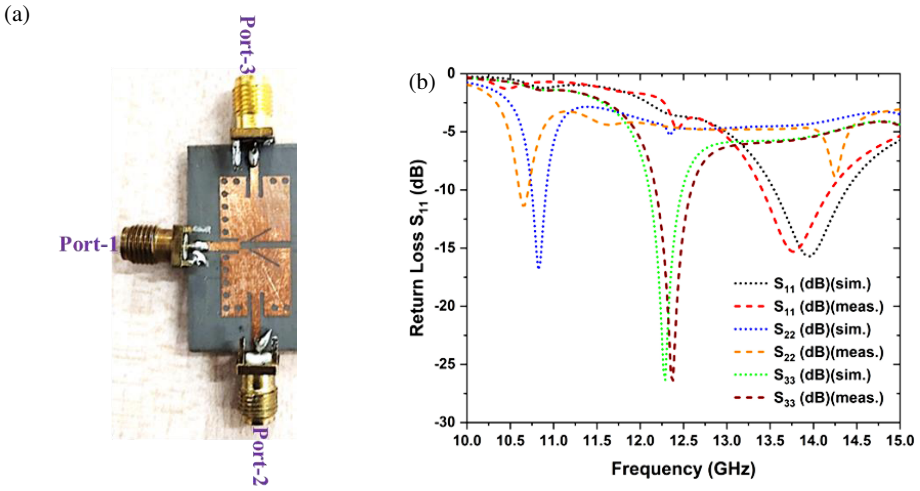

FIGURE 7. (a) Fabricated HMSIW, and (b) simulated and measured S_{11} (dB) at different ports.

TABLE 1. Performance comparison of the suggested antenna designs.

Ref.	SIW Cavity	Size in mm^3(λg^2)	Frequencies	Gain	Frequency ratio	Operation
[4]	Rectangle	48 × 76 × 21 (0.23)	2.45/3.5/4.9/5.4	3.85/5.3/5.95/5.97	2.2	Quad-band
[8]	Square	22 × 22 × 0.78 (0.17)	4.1/6.1/8.32	4.26/4.41/6.27	2.02	Tri-band
[17]	Rectangle	43.5 × 41 × 1.57 (0.55)	3.5/3.8/4.1/4.5/ 4.8/5.2/5.5/5.8	4/4.3/4.7/5.1/ 4.4/4.5/4.9/4.4	1.08	Octa-band
[18]	QMISW	35 × 40 × 1.57 (1.22)	5.2/10.81/12.16	4.12/6	2.07	Triple-band
[19]	QMSIW	24.46 × 24.46 × 1.57 (0.52)	5.2	5.58	N.A.	Uniband
[21]	HMSIW MIMO	53 × 36 × 1.57 (0.8)	3.4/4.3	5.35/6.75	1.26	Dual-band
[22]	HMSIW MIMO	82 × 82 × 1.57 (1.96)	4.43/5.39	6/6.4	1.21	Dual Band
[23]	4 PORT MIMO	27.4 × 27.4 × 1.578 (0.49)	5.2/5.8	4.85/4.6	1.11	Dual Band
[24]	Rectangle	44 × 52 × 0.76 (0.173)	2.2/2.9/3.6/4.3/5	3.5/4.5/3.9/5.7/4.9	1.4	Penta-band
[25]	Rectangle	44 × 22 × 0.76 (0.125)	2.3/2.9/5.4/6.1	4.3/3.3/6.1/4.3	2.64	Quad-band
This Work	HMSIW	22 × 11 × 1.57 (0.44)	10.82/12.28/13.95	3.97/4.62/7.55	1.13	Triple-band

the current density is less near the slot (in red color); therefore, the gain values are approximately 50% less than the gain at 13.95 GHz.

5. EXPERIMENTAL VALIDATION AND DISCUSSION

A prototype with optimal dimensions was created and tested to confirm the effectiveness of the proposed antenna design of shown in Figure 3. The manufactured prototype is shown in Figure 7(a). Further, simulated and measured return loss values are in good agreement except the shift of a few MHz at all the three resonating frequencies as depicted in Figure 7(b). This is due to the fabrication tolerances, material property variations, soldering and connector effects. Moreover, there is also slight variations in the return loss values due to various losses in fabrication, imperfect grounding and vias along with the measurement environment. Further observations in the sight mismatch between the simulated and measured bandwidths is due to the properties of the substrate and design complexity.

Figure 8 illustrates the simulated and measured 2-D far field normalized radiation patterns for the proposed antenna design. The proposed HMSIW exhibits a stable radiation pattern response at the resonant frequencies of 13.95 GHz for port-1, 10.82 GHz for port-2, and 12.28 GHz for port-3. Additionally, the antenna radiates predominantly in a broadside direction and exhibits a unidirectional radiation pattern owing to SIW-backed configuration.

Further, Table 1 presents the comparison of performance of the proposed HMSIW-SMA with the other similar research. The antenna presented in this paper has compact size as compared to those presented in [17–19, 21, 23] resonating at nearly equal frequency range in [18]. Moreover, the peak gain of the proposed HMSIW-SMA is improved as compared to the gain mentioned in other similar work. Moreover, the frequency ratio is small as compared to those provided in [4, 8, 18, 21, 22, 24, 25], which allows the design for the more efficient use of available sub-bands, enabling the allocation of more frequency channels within a given range.

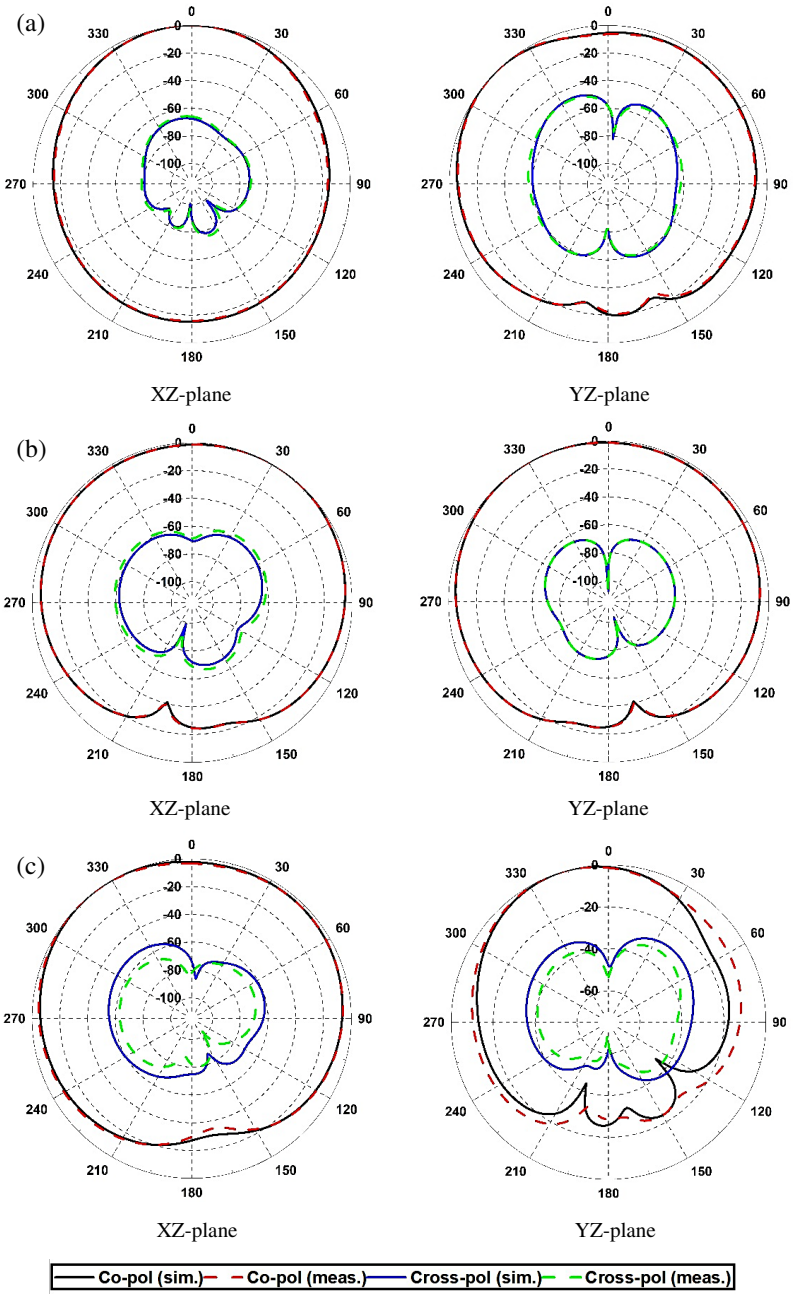

FIGURE 8. Predicted and experimented 2D far field radiation patterns of the HMSIW-SMA, (a) 13.95 GHz, (b) 10.82 GHz, (c) 12.28 GHz.

6. CONCLUSION

This article presents a compact triple band HMSIW based SMA antenna for various X- and Ku-band applications. The design is based on a slotted multiplexing antenna forming a arrow like configuration with unequal widths and lengths. The design starts with a conventional FMSIW, and further developments have been made in order to achieve the required performance parameters. The key feature of the design lies with its independent tunability of the frequency with good isolation among different ports. The proposed HMSIW-SMA exhibits several key aspects like compactness, high gain, good isolation, low frequency ratio, etc. as compared to similar reported work, which makes it suitable for various modern wireless applications.

ACKNOWLEDGEMENT

The authors would like to thank Punjabi University, Chitkara University in India, Universiti Teknikal Malaysia Melaka (UTeM), and the Ministry of Higher Education (MOHE) of Malaysia for supporting this project.

REFERENCES

[1] Ibrahim, I. M., A. J. A. Al-Gburi, Z. Zakaria, and H. A. Bakar, "Parametric study of modified U-shaped split ring resonator structure dimension at ultra-wide-band monopole antenna," *Journal of Telecommunication, Electronic and Computer Engineering (JTEC)*, Vol. 10, No. 2-5, 53–57, 2018.

[2] Al-Gburi, A. J. A., I. B. M. Ibrahim, Z. Zakaria, and N. F. B. M. Nazli, "Wideband microstrip patch antenna for sub 6 GHz and 5G applications," *Przegląd Elektrotechniczny*, Vol. 97, No. 11, 26, 2021.

[3] Chrij, D., A. Khabba, Z. E. Ouadi, L. Sellak, J. Amadid, O. Benkhadda, S. Ibnyaich, A. Zeroual, and A. J. A. Al-Gburi, "A low-cost wideband SIW antenna with bilateral slots on FR4 epoxy for Ku-band applications," *Progress In Electromagnetics Research M*, Vol. 131, 61–70, 2025.

[4] Iqbal, A., J. J. Tiang, S. K. Wong, S. W. Wong, and N. K. Mallat, "SIW cavity-backed self-quadruplexing antenna for compact RF front ends," *IEEE Antennas and Wireless Propagation Letters*, Vol. 20, No. 4, 562–566, Apr. 2021.

[5] Rammos, E. and A. Roederer, "Self-diplexing circularly polarised antenna," in *International Symposium on Antennas and Propagation Society, Merging Technologies for the 90's*, Vol. 2, 803–806, Dallas, TX, USA, 1990.

[6] Divya, G., K. Babu, I. Balakrishna, T. Addepalli, D. Z. Mohammed, Z. Zakaria, and A. J. A. Al-Gburi, "Encapsulated tri-band terahertz (THz) swiveled dielectric resonator antenna (DRA) with substrate integrated waveguide (SIW) and photonic band gap (PBG) crystal for gain enhancement," *Scientific Reports*, Vol. 15, No. 1, 29210, 2025.

[7] Jensen, M. A. and J. W. Wallace, "A review of antennas and propagation for MIMO wireless communications," *IEEE Transactions on Antennas and Propagation*, Vol. 52, No. 11, 2810–2824, 2004.

[8] Dash, S. K. K., Q. S. Cheng, R. K. Barik, N. C. Pradhan, and K. S. Subramanian, "A compact triple-fed high-isolation SIW-based self-triplexing antenna," *IEEE Antennas and Wireless Propagation Letters*, Vol. 19, No. 5, 766–770, May 2020.

[9] Kumar, A., M. Kumar, and A. K. Singh, "On the behavior of self-triplexing SIW cavity backed antenna with non-linear replicated hybrid slot for C and X-band applications," *IEEE Access*, Vol. 10, 22 952–22 959, 2022.

[10] Kumar, A. and S. Raghavan, "A self-triplexing SIW cavity-backed slot antenna," *IEEE Antennas and Wireless Propagation Letters*, Vol. 17, No. 5, 772–775, May 2018.

[11] Pradhan, N. C., S. S. Karthikeyan, R. K. Barik, and Q. S. Cheng, "A novel compact diplexer employing substrate integrated waveguide loaded by triangular slots for C-band application," *Journal of Electromagnetic Waves and Applications*, Vol. 36, No. 6, 830–842, 2022.

[12] Nandi, S. and A. Mohan, "An SIW cavity-backed self-diplexing antenna," *IEEE Antennas and Wireless Propagation Letters*, Vol. 16, 2708–2711, 2017.

[13] Priya, S., S. Dwari, K. Kumar, and M. K. Mandal, "Compact self-quadruplexing SIW cavity-backed slot antenna," *IEEE Transactions on Antennas and Propagation*, Vol. 67, No. 10, 6656–6660, Oct. 2019.

[14] Kumar, K., S. Priya, S. Dwari, and M. K. Mandal, "Self-quadruplexing circularly polarized SIW cavity-backed slot antennas," *IEEE Transactions on Antennas and Propagation*, Vol. 68, No. 8, 6419–6423, Aug. 2020.

[15] Naseri, H., P. PourMohammadi, A. Iqbal, A. A. Kishk, and T. A. Denidni, "SIW-based self-quadruplexing antenna for microwave and mm-wave frequencies," *IEEE Antennas and Wireless Propagation Letters*, Vol. 21, No. 7, 1482–1486, Jul. 2022.

[16] Jayaprakash, V., D. S. Chandu, R. K. Barik, and S. Koziel, "Compact substrate-integrated hexagonal cavity-backed self-hexaplexing antenna for sub-6 GHz applications," *IEEE Access*, Vol. 12, 54 397–54 404, 2024.

[17] Rani, A. and S. Das, "A high-lsolation SIW self-octaplexing antenna with independent frequency tuning capability," *IEEE Antennas and Wireless Propagation Letters*, Vol. 23, No. 6, 1954–1958, Jun. 2024.

[18] Jin, C., R. Li, A. Alphones, and X. Bao, "Quarter-mode substrate integrated waveguide and its application to antennas design," *IEEE Transactions on Antennas and Propagation*, Vol. 61, No. 6, 2921–2928, Jun. 2013.

[19] Jin, C., Z. Shen, R. Li, and A. Alphones, "Compact circularly polarized antenna based on quarter-mode substrate integrated waveguide sub-array," *IEEE Transactions on Antennas and Propagation*, Vol. 62, No. 2, 963–967, Feb. 2014.

[20] Caytan, O., S. Lemey, S. Agneessens, D. V. Ginste, P. Demeester, C. Loss, R. Salvado, and H. Rogier, "Half-mode substrate-integrated-waveguide cavity-backed slot antenna on cork substrate," *IEEE Antennas and Wireless Propagation Letters*, Vol. 15, 162–165, 2015.

[21] Pramodini, B., D. Chaturvedi, and G. Rana, "Design and investigation of dual-band 2 × 2 elements MIMO antenna-diplexer based on half-mode SIW," *IEEE Access*, Vol. 10, 79 272–79 280, 2022.

[22] Elobied, A. A., X.-X. Yang, N. Xie, and S. Gao, "Dual-band 2 × 2 MIMO antenna with compact size and high isolation based on half-mode SIW," *International Journal of Antennas and Propagation*, Vol. 2020, No. 1, 2965767, 2020.

[23] Almalki, M. H., A. Affandi, and A. Syed, "Design of dual-band, 4-ports MIMO antenna-diplexer based on quarter-mode substrate integrated waveguide," *International Journal of Antennas and Propagation*, Vol. 2022, No. 1, 4151038, 2022.

[24] Barik, R. K. and S. Koziel, "Design of compact self-quintuplexing antenna with high-isolation for penta-band applications," *IEEE Access*, Vol. 11, 30 899–30 907, 2023.

[25] Barik, R. K. and S. Koziel, "Highly miniaturized self-quadruplexing antenna based on substrate-integrated rectangular cavity," *IEEE Antennas and Wireless Propagation Letters*, Vol. 22, No. 3, 482–486, Mar. 2023.